Amplitude and Decay Rate Analysis of Low Level Exponentially Decaying Radio-Frequency Signals

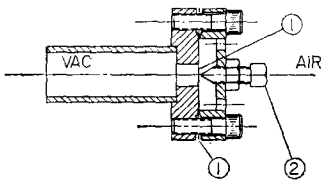

FIG. 6. A bakeable, fail-safe, pressure release. (1) 0.038 mm aluminum foil, (2) rupture pin.

Because of O-rings used in a portion of its ports, this machine is limited in its bakeability. Nevertheless, its base pressure while operating with chopping motor, beam oven, and cathode in operation is normally less than 5×10^{-8} Torr in all 3 chambers.

An added feature of the use of the trumps is that it is customary to hold the system to 10^{-5} Torr with only the trump pumping while the mercury trapped on the LN traps is being released back to the diffusion pumps by warming the traps to room temperature. This can be done as often as required without harming indirectly heated cathodes, etc., within the system. A second virtue of trumps involves their usefulness during interruptions of electrical power, planned or otherwise.

Trump D

Trump D was designed to have somewhat superior characteristics to the previous models. At this writing testing has not been completed. Generally it can be stated that the ability of all of the trumps is limited by the degree to which the zeolite can be cooled. It is expected that colder surfaces will be even more successful than those at LN temperature. While the externally cooled trumps are probably the most easily constructed and have the lowest effective temperatures, the internally cooled trumps are more efficient in LN use. Heat shields must be used effectively in these trumps. Both can be heated easily for bakeout with heater socks or tapes. The internally heated trumps can be heated with immersion heaters. Undervolting is preferable for longer heater life in this usage.

SAFETY

It should be noted that excessive pressures result if a closed, loaded, LN-cooled trump is allowed to warm to room temperatures. A clean pressure release which is used extensively with trumps and commercial pumps is shown in Fig. 6.

The 0.025–0.076-mm aluminum diaphragm can be caused to rupture at a useful range of pressures by adjustment of the screw point. A 0.038-mm, 1145 soft aluminum foil ruptures at 60–80 psi without this puncture pin.

ACKNOWLEDGMENTS

Since these designs have evolved over an extended period of time to implement other areas of research, many people have contributed ideas. E. C. Popp and co-workers constructed one of the first internally cooled units for use as a pump. It was only partially successful and was unfortunately abandoned due to inadequate heat shielding and the resulting higher base temperature of the zeolites. Joseph Fabyan, John Kinney, and Russel Niver have contributed toward the currently used models.

THE REVIEW OF SCIENTIFIC INSTRUMENTS VOLUME 36, NUMBER 3 MARCH 1965

Amplitude and Decay Rate Analysis of Low Level Exponentially Decaying Radio-Frequency Signals*

HOWARD C. BERG†
Lyman Laboratory of Physics, Harvard University, Cambridge, Massachusetts
(Received 6 November 1964)

A method is described which allows routine measurements of the relative amplitudes and absolute decay rates of low level exponentially decaying radio-frequency signals to be made to within an accuracy of 1%. The signals are converted to audio frequency, narrow banded, rectified, and integrated over two successive periods of time. The theory of the measurement, which is given in detail, shows how the analysis can be made in the presence of noise which is white over a frequency bandwidth large compared to the inverse decay times. The general features of the circuits are described, and a schematic is given for a nearly ideal full-wave linear rectifier.

INTRODUCTION

WE will discuss in this paper an accurate electronic method for the two-parameter analysis of exponentially decaying, low level, radio-frequency signals. The method was developed for an experiment with the atomic hydrogen maser[1,2] in which the relative amplitudes and absolute decay rates of a large number of exponentially decaying 1420-Mc signals were measured at a power level of about 10^{-14} W. The signals, which originated from the stimulated emission of about 10^{10} hydrogen atoms, could be generated at will by the application of a microwave pulse.

* Work supported by the National Science Fundation and the U. S. Office of Naval Research.
† Junior Fellow, Harvard Society of Fellows.

[1] H. C. Berg, Phys. Rev. (to be published).
[2] H. C. Berg, thesis, Harvard University (1964, unpublished).

Depending upon the choice of certain experimental parameters, the amplitudes and decay rates ranged from 1 to 10 (on a relative scale) and from 1 to 10 sec^{-1}, respectively.

This is a rather special problem, but the solution which will be given here can be extended to the reduction of any exponentially decaying signal in the presence of noise which is white over a frequency bandwidth large compared to the inverse decay time. The sections of the paper which follow give a general outline of the method, develop the theory of the measurement, describe briefly some features of the circuits, and summarize the performance obtained in the maser experiment. Accurate amplitude and decay rate measurements can be made only if proper consideration is taken of the effects of the noise.

GENERAL SCHEME

The method is based on the integration of each of a train of N signals over two successive periods of time. The general features of the system are shown in Fig. 1. The signal is detected by conventional microwave techniques and amplified about 70 dB by a variable-gain broadband i.f. amplifier. The i.f. output is converted linearly to a lower frequency and the bandwidth is limited by a tuned *RLC* Lorentzian filter. The filter ouput, Fig. 2, is rectified by a nearly ideal full-wave linear rectifier and presented to two relays which feed two identical integrators. The relays are closed on the command of a relay control circuit which uses as a time reference a 100-cps pulse train from an electronic counter. At time 0, a microwave pulse is sent to the maser, and a signal is generated. At time t_1, relay 1 is closed. At time t_1+t_2, relay 1 is opened and relay 2 is closed. At time t_1+3t_2, relay 2 is opened. The signal is integrated over two successive periods of time, t_2 and $2t_2$, beginning at time t_1. This pulsing and integrating process is repeated N times ($10<N<120$, depending upon the signal-to-noise level), and the two integrator outputs a_1 and a_2 are recorded. The pulse generator is turned off, and the entire procedure is repeated. In this manner, the information contained in a train of N signals and N noise samples is reduced to four voltages, a_1, a_2, a_{1n}, and a_{2n}.

THEORY

The converter output frequency is large compared to the filter bandwidth, and the filter bandwidth is large compared to the largest signal decay rate encountered in the experiment (5.76 kc, 150 cps, and 10 sec^{-1}, respectively). If the input signal to a Lorentzian filter tuned to the angular frequency ω is $\exp(-\gamma t)\cos\omega t$, then it can be shown that the output signal is

$$[\Gamma/(\Gamma-\gamma)][1-\exp(-\Gamma t+\gamma t)]\exp(-\gamma t)\cos\omega t, \quad (1)$$

where Γ is a number proportional to the filter width.[3] If Γ is sufficiently large, the factor $\Gamma/(\Gamma-\gamma)$ is nearly 1; after an interval of time, long compared to $(\Gamma-\gamma)^{-1}$, the output signal decays at the input decay rate γ. Once γ has been measured, the initial signal amplitude can be obtained by extrapolating exponentially back to $t=0$ and by multiplying the $t=0$ amplitude by $(\Gamma-\gamma)/\Gamma$.

If a rectangular signal of amplitude A, length T, and frequency ω is fed into the filter ($T\gg\Gamma^{-1}$), it can be shown that the output increases exponentially at a rate Γ to amplitude A, and then after a time T, decays again at a rate Γ. If a test signal of this kind is used, Γ can be measured. (For the maser experiment, $\Gamma=488$ sec^{-1}.)

The time t_1 is chosen to be several times larger than Γ^{-1}, so the integration begins after the filter transient has damped out. This can be seen in Fig. 2(b). The disturbance at the beginning of the signal is due to the leakage of part of the pulse power into the signal line. The pulse is normally delivered to the maser and to the detector in such a way that the net pulse power at the balanced mixer is small. The microwave pulse is only 0.003 sec wide, but the response to the pulse at the filter output grows and decays at the rate Γ. The time t_1 occurs 0.0012 sec after the first step of the monitor trace ($t_1=0.0212$ sec).

In practice, the filter input signal contains noise which is white over a frequency bandwidth large compared to the filter width. For $t>t_1\gg\Gamma^{-1}$, the output can be expressed in the form

$$y_{(t)}=P_{(t)}\cos\omega t+x_{c(t)}\cos\omega t-x_{s(t)}\sin\omega t, \quad (2)$$

where $P_{(t)}=[\Gamma/(\Gamma-\gamma)]\exp(-\gamma t)$, and $x_{c(t)}$ and $x_{s(t)}$ are sample functions of a stationary, narrow band, Gaussian

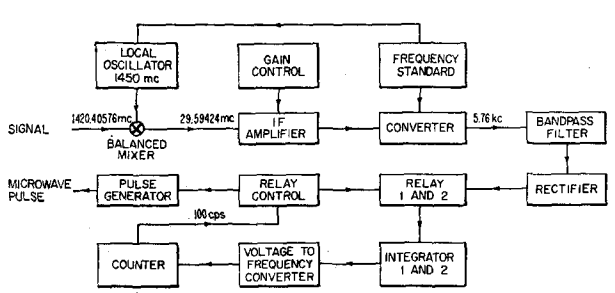

FIG. 1. Pulsed signal analysis system.

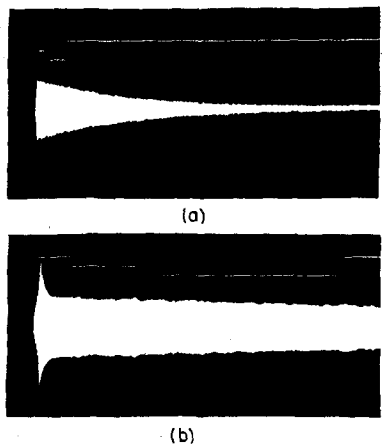

FIG. 2. (a) Oscilloscope display of the bandpass filter output. The upper trace monitors the state of the relay control circuit. The steps occur at 0.02, 0.07, and 0.17 sec. (b) A similar signal displayed at ten times the sweep speed. The experimental conditions are the same except that a small part of the microwave pulse power has leaked into the signal line. The shape of this disturbance is determined by the filter response time.

[3] C. W. Helstrom, *Statistical Theory of Signal Detection* (Pergamon Press, Inc., New York, 1960), Chap. 1.

random process.[4] The random variables which refer to the possible values of $x_{c(t)}$ and $x_{s(t)}$, namely x_{ct} and x_{st}, are independent Gaussian random variables. We may also write

$$y_{(t)}=[(P_{(t)}+x_{c(t)})^2+x_{s(t)}^2]^{\frac{1}{2}}\cos(\omega t+\varphi_{(t)}), \quad (3)$$

where

$$\varphi_{(t)}=\tan^{-1}[x_{s(t)}/(P_{(t)}+x_{c(t)})]. \quad (4)$$

The rectifier is a synchronous full-wave switch with the transfer function $+1$ if $y_{(t)}>0$ and -1 if $y_{(t)}<0$. Since the filter is narrow banded, $x_{c(t)}$, $x_{s(t)}$, and $\varphi_{(t)}$ are slowly varying functions of time compared to the function ωt. The time integral of the rectified cosine function over one switching period is approximately constant. The average value of the rectifier output over this period is proportional to

$$[(P_{(t)}+x_{c(t)})^2+x_{s(t)}^2]^{\frac{1}{2}}, \quad (5)$$

where t is the time, say, of the middle of the period. (We drop the proportionality constant, since only relative amplitudes are of concern.) If a large number of signals are integrated, the integrator extracts the ensemble average

$$S_{(t)}=\langle[(P_{(t)}+x_{ct})^2+x_{st}^2]^{\frac{1}{2}}\rangle_{\text{av}}, \quad (6)$$

where we normalize the average to $N=1$. If we integrate only the noise, the integrator extracts the ensemble average

$$D=\langle[x_{ct}^2+x_{st}^2]^{\frac{1}{2}}\rangle_{\text{av}}. \quad (7)$$

The ensemble averages can be computed from the joint probability distribution function for x_{ct} and x_{st} and from the distribution function for $(x_{ct}^2+x_{st}^2)^{\frac{1}{2}}$. We obtain

$$S_{(t)}\simeq P_{(t)}[1+\sigma_x^2/2P_{(t)}^2+9\sigma_x^4/8P_{(t)}^4+\cdots] \quad (8)$$

and

$$D=(\pi/2)^{\frac{1}{2}}\sigma_x, \quad (9)$$

where σ_x is the standard deviation of the Gaussian distribution for x_{ct} and x_{st}, and we have assumed $P_{(t)}>\sigma_x$ and expanded the square root. In terms of the integrated time-average noise value D,

$$S_{(t)}\simeq P_{(t)}[1+D^2/\pi P_{(t)}^2+9D^4/2\pi^2P_{(t)}^4+\cdots]. \quad (10)$$

For the noise levels encountered in the maser experiment $(D/P_{(t)})^4$ and higher order terms can be neglected, provided the integration is completed before $D/P_{(t)}$ becomes large. (t_2 is chosen so that $D/P_{(t_1+3t_2)}<0.3$.) If we substitute for $P_{(t)}$ the expression $b\exp(-\gamma t)$, then

$$S_{(t)}\simeq b\exp(-\gamma t)[1+(D^2/\pi b^2)\exp(2\gamma t)]. \quad (11)$$

Suppose N signals are integrated. The first integrator charges to a voltage a_1, which is N times the time integral of Eq. (11) from t_1 to (t_1+t_2),

$$a_1=\frac{Nb(1-\delta)\exp(-\gamma t_1)}{\gamma}\left[1+\frac{D^2}{\pi b^2\delta}\exp(2\gamma t_1)\right], \quad (12)$$

where

$$\delta=\exp(-\gamma t_2). \quad (13)$$

The second integrator charges to a voltage a_2, which is N times the time integral of Eq. (11) from (t_1+t_2) to (t_1+3t_2),

$$a_2=\frac{Nb\delta(1-\delta^2)\exp(-\gamma t_1)}{\gamma}\left[1+\frac{D^2}{\pi b^2\delta^4}\exp(2\gamma t_1)\right]. \quad (14)$$

(We assume both integrators charge to 1 V after integrating a 1 V signal 1 sec.) If we integrate only the noise, the first integrator charges to a voltage $a_{1n}=Nt_2D$ and the second integrator charges to a voltage $a_{2n}=2Nt_2D$, so that

$$D=(1/3Nt_2)(a_{1n}+a_{2n}). \quad (15)$$

Computing the ratio a_2/a_1 and discarding terms of order $(D/b)^4$, we find

$$\delta^2+\delta-(a_2/a_1)(1-F)=0, \quad (16)$$

where

$$F=[(1-\delta^3)/\delta^4](D^2/\pi b^2)\exp(2\gamma t_1). \quad (17)$$

The required root of Eq. (15) is

$$\delta=\tfrac{1}{2}[1+(4a_2/a_1)(1-F)]^{\frac{1}{2}}-\tfrac{1}{2}. \quad (18)$$

In terms of F, γ, and a_1,

$$b=\gamma a_1\exp(\gamma t_1)/N(1-\delta)[1+\delta^3F/(1-\delta^3)]. \quad (19)$$

Equations (13) and (17–19) can be solved by iteration. In zero order, F is taken equal to 0. (This is the correct solution in the limit of large signal-to-noise ratios.) The computed values of δ, γ, and b are used to compute F to first order, and so on. The initial relative signal amplitude is then given by $b(\Gamma-\gamma)/\Gamma$. In practice, higher i.f. amplifier gains are required for the analysis of lower level signals, and the relative amplitude values are normalized to a given amplifier gain setting. An IBM card is punched for each signal and the calculations are done on an electronic computer.

For signals which are very much smaller than the noise, the expression analogous to Eq. (8) is

$$S_{(t)}\simeq D[1+\pi P_{(t)}^2/8D^2]. \quad (20)$$

If the bandpass filter output is repeatedly photographed, the noise is not averaged in the same way that it is by an integrator, because everything but the peak signal washes out. The approximate average peak value of Eq. (5) is

$$(P_{(t)}+u)[1+\tfrac{1}{2}u^2/(P_{(t)}+u)+\cdots]\simeq P_{(t)}+u, \quad (21)$$

where u is a number larger than the average rms value of x_{ct} or x_{st}. The approximate average peak value of the noise is $\sqrt{2}u$. If the photograph is to be fit by a standard exponential curve, the baseline for the fit should be chosen to be about 0.7 times the average peak value of the noise.

[4] W. B. Davenport and W. L. Root, *An Introduction to the Theory of Random Signals and Noise* (McGraw-Hill Book Company, Inc., New York, 1958), p. 158.

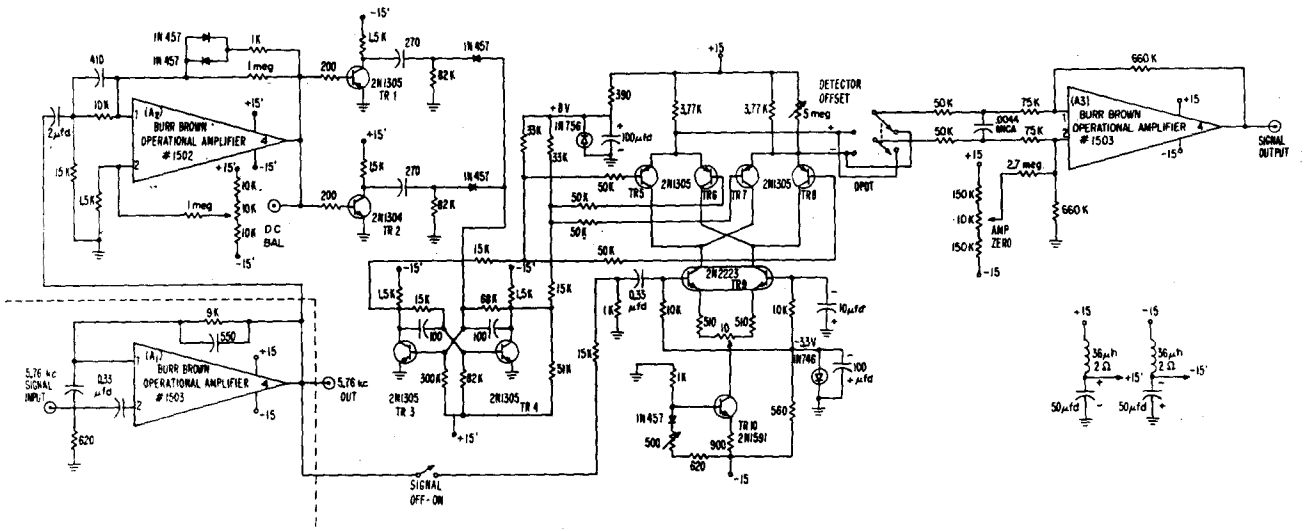

FIG. 3. Rectifier circuit. The capacitance values are given in $\mu\mu$F unless otherwise noted. The resistors which appear as pairs in the differential switch TR5–TR9 and in the amplifier A_3 are matched to 0.1%. A±15-V regulated power supply is required.

The filter output could be passed through a square-law device rather than a linear rectifier. In this case, Eqs. (11)–(19) are valid following the transformation $b \rightarrow b^2$, $\gamma \rightarrow 2\gamma$, $D=0$, $a_1 \rightarrow a_1 - a_{1n}$, $a_2 \rightarrow a_2 - a_{2n}$, and $F=0$. The filter amplitude correction factor $(\Gamma-\gamma)/\Gamma$ is applied as before.

CIRCUITS

The circuits have been given in detail elsewhere.[2] We include in this section only those features of general interest.

The converter is linear to within a few tenths of a percent over the required signal range. This is easy to do with conventional transistor tuned circuits by mixing in two steps with fixed high power standard signals (30 Mc and 400 kc in the maser example). To eliminate interference from pickup and noise, the first mixer stage is preceded by a filter tuned to the i.f. frequency which has a bandwidth just narrow enough to suppress the components of the i.f. output at the first standard frequency.

The rectifier is linear to within 0.1% over a peak-to-peak signal input range of 1 V to 3×10^{-3} V. The latter value is at least 20 times smaller than the smallest noise signals encountered. Since a circuit of this nature has many applications, we give its schematic diagram in Fig. 3. A_1 is a gain 16 broadband ac amplifier corrected to give zero phase shift at 5.76 kc. A_2 is a logarithmic amplifier with a small signal gain of 100. The output of flip-flop TR3–TR4 is synchronous with the zero-crossing of the input signal, and it drives the DPDT transistor switch in the collector circuit of the differential amplifier TR9. The high frequency components of the TR9 output signal are smoothed by an *RC* circuit, and the signal is referred to ground by the gain 10 dc difference amplifier A_3. The low impedance output signal of this amplifier is fed to the relay inputs.

If the Signal Off-On switch is turned off, only the switching transients appear at the output of TR9. When the circuit has warmed up, an audio oscillator input is used, and the Detector Offset control and the controls connected with the constant current supply TR 10 are adjusted so that the dc component of this output is approximately 0 V. The final tune-up is performed periodically in the following way: The signal input is removed, and A_2 is balanced by setting the dc Bal control so that the A_2 output is about 0.001 V (not critical). The signal input is connected again (at least a noise signal is required to drive the switch circuits) and the Signal Off-On switch is turned off. The Detector Offset and Amp Zero controls are adjusted so the rectifier output signal averages to less than 0.001 V.

The relays are reed relays chosen for minimum bounce (GE CR120G30103). There is a 0.0012-sec delay between the time the coils are activated and the time the contacts close, so the opening delay is matched to this value by placing a diode-resistor shunt across the coils. The time t_1 is then 0.0012 sec larger than the 0.02 sec set by the relay control; the time t_2 is not changed.

The relay control provides for a range of t_2 times, including 0.05, 0.10, 0.15, and 0.20 sec. Each is an even multiple of a 60-cps period, so 60-cps pickup is rejected by the integrators. The $t_2=0.05$ sec control sequence is illustrated by the upper traces of Figs. 2(a) and 2(b). If the signals are not exponential, this can be shown by repeating the analysis at different t_2 settings.

The integrators are conventional dc amplifier circuits which use matched $10^5\ \Omega$ input resistors, matched 20-μF Mylar capacitors, and regenerative feedback to compensate for leakage. The circuits must hold their charge long enough when the input relays are open that read-in and read-out time errors are small.

PERFORMANCE

Nearly a thousand signals were analyzed with this system with ease. The accuracy of the analysis was checked at high signal-to-noise levels by a photographic curve-fitting technique, and the two methods agreed to within the precision that the photographs could be read (to a fraction of a percent). The noise correction was checked by analyzing a given maser signal for its decay rate after inserting different attenuators in the signal line. The values found over a $D/P_{(t_1+3t_2)}$ range of 0.1 to 0.4 agreed to within 1%.

ACKNOWLEDGMENTS

The author is indebted to Professor Norman F. Ramsey, who guided and supported the hydrogen maser research throughout its course, to William Bossert, for discussions of data analysis and the design of the computer program, and to the National Institutes of Health for a predoctoral fellowship during the years 1959–1963.

THE REVIEW OF SCIENTIFIC INSTRUMENTS VOLUME 36, NUMBER 3 MARCH 1965

Precision Measurement of Lattice Imperfections with a Photographic Two-Crystal Method

J. A. BEARDEN AND ALBERT HENINS
Department of Physics, The Johns Hopkins University, Baltimore, Maryland
(Received 28 September 1964; and in final form, 16 October 1964)

A photographic two-crystal spectrometer method employing the penetrating W $K\alpha_1$ line has been developed. In the present investigation this technique was used to test large crystals with areas up to 25×50 mm in reflection and volumes up to 25×3.5×5 mm in transmission; angular deviations in the lattice as small as 0.5″ were detected. The first crystal was a nearly perfect calcite 30×70×10 mm used in the second order and located 100 cm from the tungsten x-ray tube and also 100 cm from the second crystal (one tested) which was usually set in the −2 order. The 200-cm distance from the focal spot to the second crystal separated the $\alpha_1\alpha_1$ lines and allowed the α_2 line to be blocked out when testing a calcite crystal. In most tests the crystals were of different d_∞'s, and a small dispersion resulted, but essentially gave the rocking curve expected from the Darwin-Prins single-crystal diffraction pattern. A NaI detector and a scaler were used to locate the peak and half-intensity points of the rocking curve. A photographic film was placed between the detector and test crystal, and an exposure of 5 to 20 min was made at each of the three positions. Structure in the image gave a measure of the imperfections and their location on the surface of the test crystal. Approximately 100 samples of calcite, quartz, silicon, and germanium crystals have been tested, of which only six or seven approximated perfection. The sensitivity and speed of the method appear superior to any thus far developed, and it provides not only an excellent test procedure for selecting crystals for precision x-ray wavelength measurements and high resolving power studies, but also for further perfecting synthetic crystal-growing techniques.

INTRODUCTION

THE measurement of x-ray wavelengths[1] with selected crystals has attained a precision of approximately 1 ppm (parts per million) and for γ rays[2] the order of 10 ppm. The primary limitation in both cases is due to the fact that most large crystals are not single perfect geometrical structures, but are composed of many "perfect" elements slightly misoriented. The required size of a crystal depends on the type of x-ray spectrometer employed, its use in transmission or reflection, and upon the wavelength measured. In transmission, γ-ray measurements use crystals[2] of the order of 20×20×20 mm. Smaller crystals may be used for x rays, e.g., the W $K\alpha_1$ beam may be 5×3 mm and require a crystal of 5 mm in thickness. Curved and double-crystal spectrometers require large perfect crystals. Longer wavelengths are usually measured in reflection, and the double-crystal measurement of the Mo $K\alpha_1$ line diffracted in the first order with an x-ray beam width of 3 mm (focal spot size) requires crystals of approximately 30 mm in length.

Peaks[1,3] of symmetrical lines can be located within approximately 0.001 their observed width. In the case of γ rays and short x rays this amounts to a few hundredths of a second in angle, and the measurement of Bragg angles has attained the same order of precision. Ideally for the best wavelength measurements the crystal lattice perfection should be of this accuracy. If large perfect crystals can not be obtained, then the x-ray beam must be restricted and alignment procedures[1] made such that the best small area of the crystal is used. In studies of line shapes, absorption edges, etc, the natural widths are of the order of 10 to 100″, and the same crystal area is used for the entire measurement, thus permitting the use of

[1] J. A. Bearden, Albert Henins, J. G. Marzolf, W. C. Sauder, and J. S. Thomsen, Phys. Rev. 135, A899 (1964).
[2] J. W. Knowles, Can. J. Phys. 40, 257 (1961).
[3] J. W. Knowles, International Conference on Nuclear Physics with Reactor Neutrons (AEC) ANL-6797, edited by F. E. Throw, p. 165.